Nano Science and Nano Technology
An Indian Journal

Trade Science Inc.

➤ *Full Paper*

Metal sulfide WS$_2$ nano-films synthesis and characterization : A focus on cost and mechanical properties enhancement

K.M.Boubaker
ESSTT/ 63 Rue Sidi Jabeur 5100, Mahdia, (TUNISIA)
E-mail: math_physics2008@yahoo.fr

ABSTRACT

WS$_2$ nano films have been elaborated from WO$_3$ layers grown on glass substrates using a simple and cheap technique. Several characterization means including classical and original protocols, like Vickers micro-hardness test and Amlouk-Boubaker opto-thermal expansivity ψ_{AB} analyses have been carried out. The results showed that the finally fabricated films contained only WS$_2$. This feature gives a meaningful advantage to the process in the matter of product purity, as long as similar ones yielded undesirable products such as WO$_y$S$_{2-y}$ and WO$_y$S$_2$.
© 2012 Trade Science Inc. - INDIA

INTRODUCTION

WS$_2$ is one of the most known materials due to photovoltaic, lubricous and tribological properties[12,22,26,27]. Several routes have been established for the synthesis of this compound[13,14,4,5,7] under its two types (type-I, grown with c-axis parallel to the deposition surface and type-II with c-axis perpendicular to surface).The present study focuses on a two-step fabrication process starting from a sprayed WO$_3$ material. The idea of using this sprayed precursor is not new.[24]used mechanically assisted ultrasonic spray pyrolysis deposition technique (USP) to deposit tungsten oxide thin films by spraying 2·0 mM aqueous ammonium metatungstate solution onto amorphous glass substrates kept at 250°C. A major inconvenient of this method consists of the need of a subsequent annealing at 400°C for a considerable duration. Ten years later[12]

succeeded to implement a claimed simple solvo-thermal cum chemical reduction route, with sodium tungstate (Na$_2$WO$_4$) and cetyl trimethyl ammonium bromide (C$_{19}$H$_{42}$NBr) as main reactants. The process didn't seem to be simple as it involved some complicated steps as sealing tubes and submerging them into water baths at 80°C for more than 80 hours. The need of repeated centrifugation and washing with distilled water was also an additional difficulty. In order to compare the actual protocol to those cited above, along with similar methods used by[20,18] temperature ranges, cost and effects on films microhardness have been discussed.

EXPERIMENTAL

Precursor Tungsten oxide thin films were prepared at a substrate temperature of 500°C using (NH$_4$)$_2$WO$_4$. 1.0 µm-thick thin films were obtained by performing

Full Paper

deposition using a freshly prepared 0.01M solution. Thickness was estimated using the protocol proposed by[4,5].

After a short annealing treatment Tungsten oxide thin films were annealed in sulfur-rich atmosphere at 550° C inside a tube sealed under vacuum (10^{-2}-10^{-3} Pa). The chemical process which occurs after the chosen duration of 2 hours is likely to be described by the the global reaction:

$$2S_{sol.} + WO_3 \rightarrow WS_2 + \frac{3}{2}O_2$$
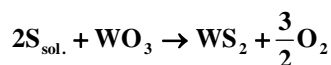
As stated before, a similar process has been proposed earlier[18,29], but with a major inconvenient which consists of two increment of high temperature (760 and 920° C) along with the unavoidable appearance of an intermediary compounds such as WO_yS_{2-y}[17,8] and tungsten oxy-sulphide WO_yS_2[21] Nevertheless, the present protocol uses a simple spray setup at relatively low temperatures, and hence leads to a lower cost.

The schematic representation of the whole process is summarized in Figure 1.
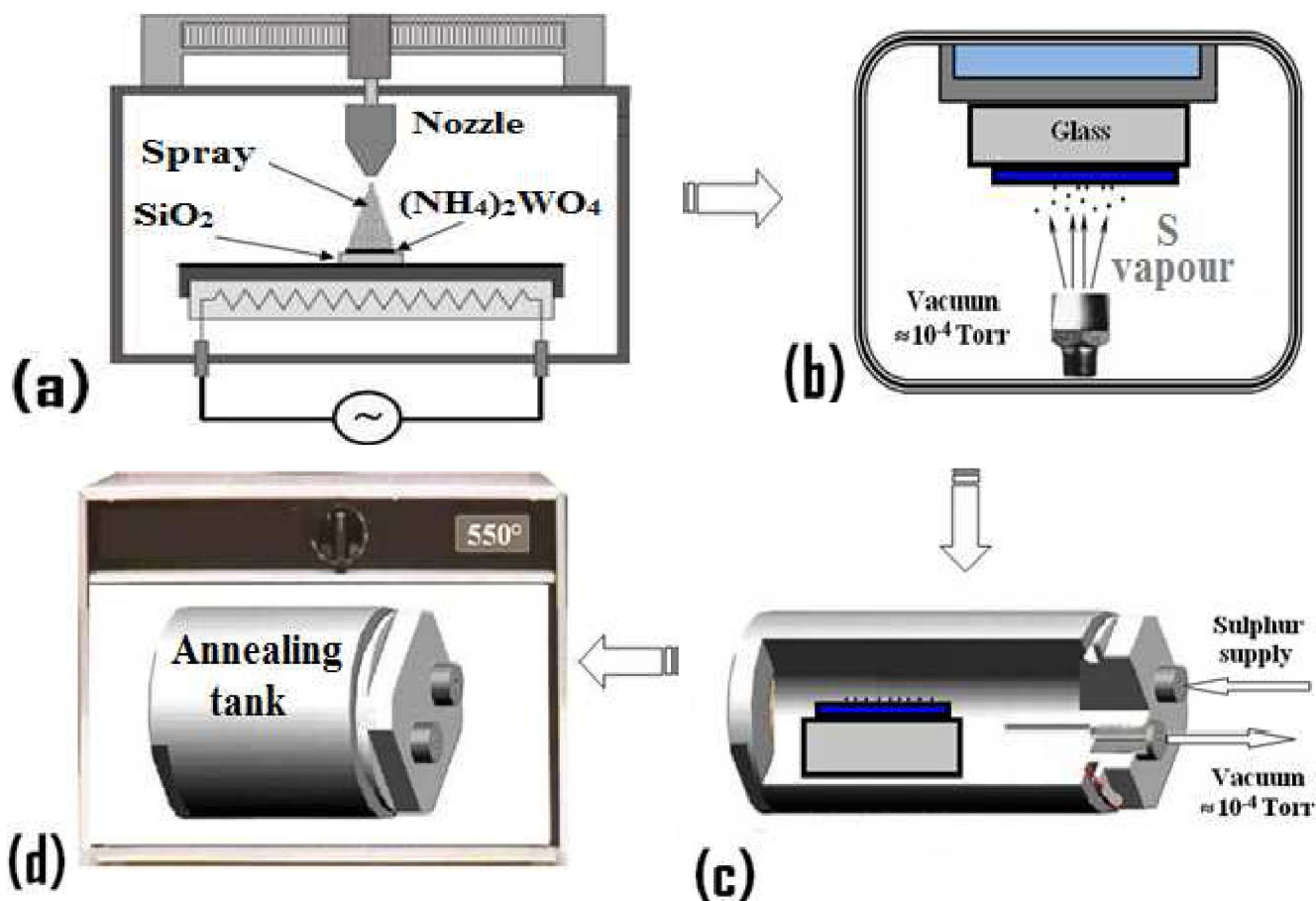
(a) Deposit of sprayed WO_3 on SiO_2 substrate (b) Sulphur vaporization under vacuum (c) Sealing in a sulphured medium (d) Annealing phase.
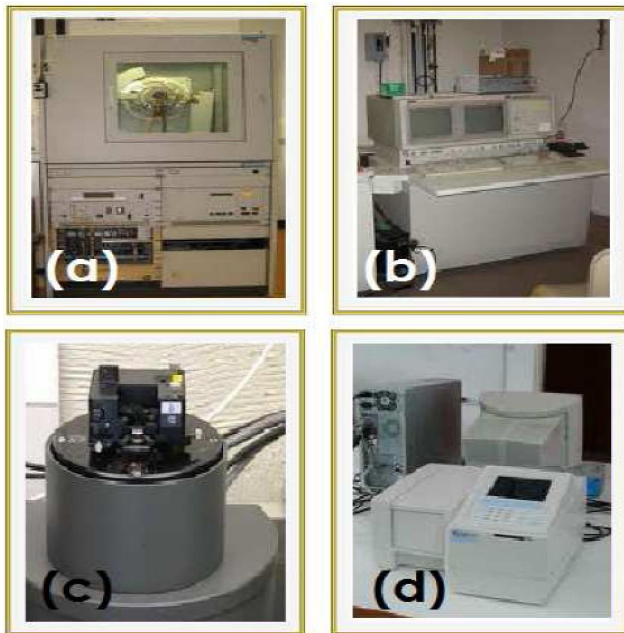
Figure 1 : WS₂ nano-layers elaboration process.

RESULTS AND DISCUSSION

The obtained WO_3 and WS_2 films were conjointly investigated by X-ray diffractometry (XRD) using a Siemens D500 Diffractometer (Figure 2-a) equipped with monochromatic CoKα radiation (λ= 1,7903 Å). The acceleration voltage was 45 kV and the current intensity was 40 mA. Morphological aspects and surface topography of the films were examined by scanning electron microscopy (SEM) using a JEOL 6400 high-resolution apparatus, with beam voltages ranging from 0.2kV to 40 kV and beam currents from 10 pA to 10 µA (Figure 2-b) and by atomic force microscopy (AFM : Park Scientific Instrument) in contact mode (Figure 2-c). Finally, optical measurements of the λ-dependent

transmittance and the reflectance were carried out in the wavelength range λ (300 to 2500 nm) using unpolarized light in normal incidence by means of a common spectrophotometer (Figure 2-d) equipped with an integrating sphere (LISR 3200). The spectrophotometer consists of double-beam monochromator (UV-2OOS, Shimazdu apparatus) with monochromatization performed by two flat silicon crystals in Laue diffraction on

(a) XRD Diffractometer. (b) Scanning electron microscopy (SEM) setup. (c) Atomic force microscopy (AFM) setup. (d) Optical measurements spectrophotometer.

Figure 2 : Synopsis of the experimental setups.

the (111) plane in a wide wave-length.

The obtained WO_3 and WS_2 films were conjointly investigated by X-ray diffractometry (XRD) using a Siemens D500 Diffractometer equipped with monochromatic $CoK\alpha$ radiation (λ= 1,7903 Å). The acceleration voltage was 45 kV and the current intensity was 40 mA. Morphological aspects and surface topography of the films were examined by scanning electron microscopy (SEM) and by atomic force microscopy (AFM). Finally, Optical measurements of the λ-dependent transmittance and the reflectance were carried out in the wavelength range λ (300 to 2500 nm) using unpolarized light in normal incidence by means of a UV 3100 S double-beam spectrophotometer equipped with an integrating sphere "LISR 3200". Barium sulphate and air were taken as references for the reflection and transmission measurements respectively within a <100-
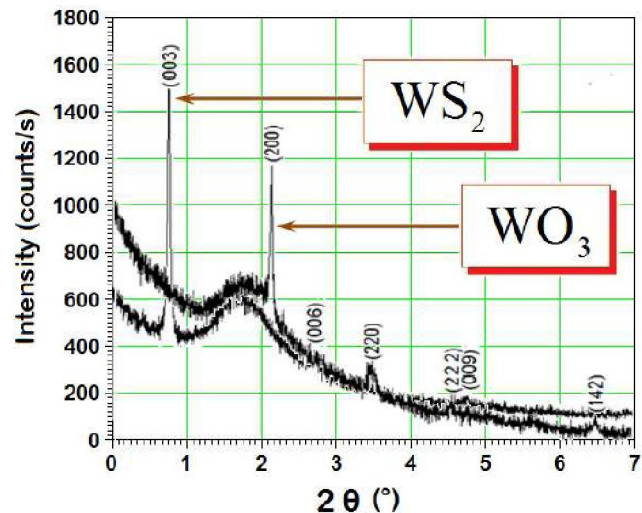

Figure 3 : Conjoint XRD Diagrams of WO_3 and WS_2 nanofilms.

1800 nm> wavelength range.

XRD patterns of both finally produced WS_2 and WO_3 precursor, gathered in Figure 3, show that the initially deposited WO_3 layers monitor an obvious preferred orientation of the crystallites with respect to the (200) reflection direction which contrasts with tungsten disulfide XRD peaks as stated by[28,19] Their thorough investigation confirmed that similar WS_2 material are crystalline with predominantly hexagonal (002) texture which monitors basal planes with c-axis orientated parallel to the substrate surface [(100) and (101) reflections]

From another side, AFM and SEM patterns of the WO_3 and WS_2 films (Figure 4 and 5, respectively) depict a drastic decrease of the mean surface roughness (from around 41.0 nm for WO_3 to approximately 6.0 nm for WS_2). This change is confirmed by the noticed formation of sulphured clusters perpendicularly to the glass substrate plane, which results in better optical transparency as already recorded by[19,12,22] For giving more evidence to the effectiveness of the protocol, two additional characterization tests have been carried out. The tests concern Vickers micro-hardness and the Amlouk-Boubaker opto-thermal expansivity ψ_{AB}[1-3,10,11,23]. According to ASTM E-384, EN ISO 6507, and ASTM E-92 standards, Vickers Hardness test specifies making indentation with a range of loads using a diamond indenter which is then measured and converted to a hardness value. This test was considered to be very useful for testing on a wide type of materials, including metals, and ceramics, nevertheless, its appli-

Full Paper

cation to layered structure is very recent[20]. The load-independent hardness measurements have been performed by a standard Micro-Hardness Vickers (*Hv*)
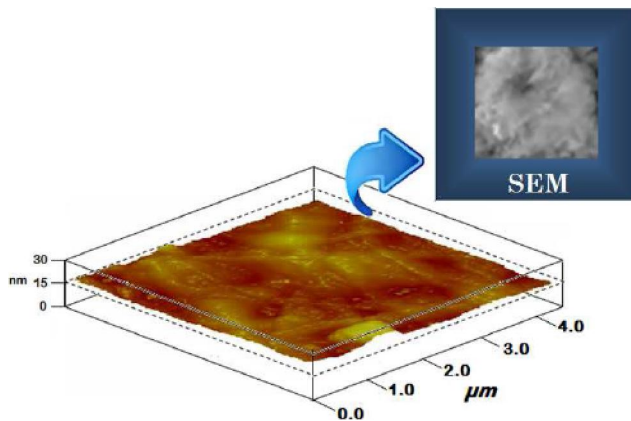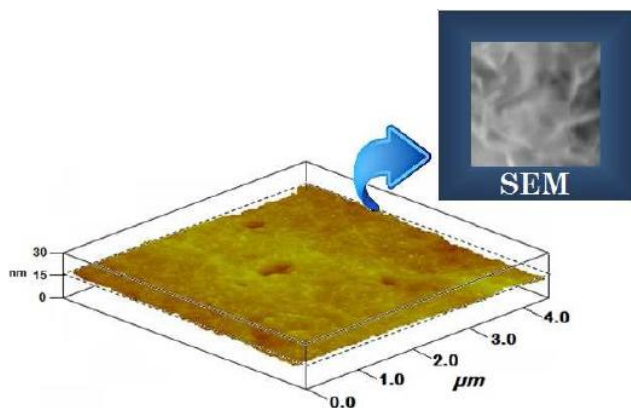

Figure 4 : WO₃ nano-films AFM and SEM images.

Figure 5 : WS₂ nano-films AFM and SEM images.

apparatus.

In precedent studies[2,10,23], the Amlouk-Boubaker opto-thermal expansivity ψ_{AB} has been defined by (Eq. 1)

$$\psi_{AB} = D / \hat{\alpha} \qquad (1)$$

where *D* is the thermal diffusivity and ** is the already defined effective absorptivity, defined in APPENDIX. This parameter, expressed in $m^3 s^{-1}$, is assimilated to a 3D expansion velocity of the transmitted heat inside the material.

The evolution of the values of the Vickers Hardness and Amlouk-Boubaker opto-thermal expansivity ψ_{AB}, for the two studied layers, are gathered in Figure 6. The evolution monitored in Figure 6 is in concordance with the precedent analyses. In fact, a decrease in the Amlouk-Boubaker opto-thermal expansivity ψ_{AB} along with an increase in Vickers Micro-Hardness confirms the appearance of a better organization inside the newly

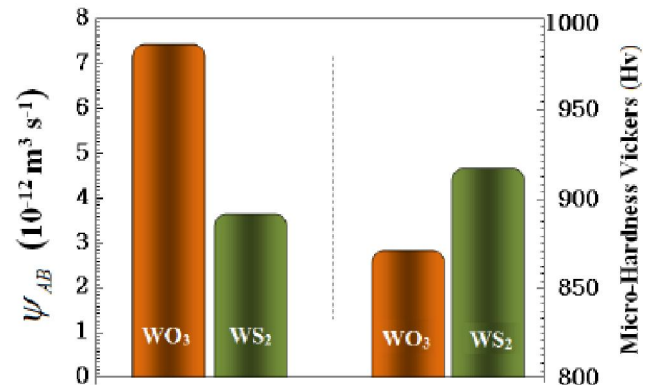established crystallites of tungsten sulphide clusters. Moreover, tungsten-related clusters patterns were found

Figure 6 : Evolution of Micro-Hardness Vickers (Hv) and Amlouk-Boubaker opto-thermal expansivity ψ_{AB}

in good agreement with those published by[16,9,25].

APPENDIX

The effective absorptivity $\hat{\alpha}$, is the mean normalized absorbance weighted by $I(\tilde{\lambda})_{AM1.5}$, the solar standard irradiance, with $\tilde{\lambda}$: the normalized wavelength:

$$\begin{cases} \tilde{\lambda} = \dfrac{\lambda - \lambda_{min}}{\lambda_{max} - \lambda_{min}} \\ \lambda_{min} = 100.0 \, nm \; ; \lambda_{max} = 1800.0 \, nm. \end{cases} \qquad (A.1)$$

and:

$$\hat{\alpha} = \frac{\int_0^1 I(\tilde{\lambda})_{AM1.5} \times \alpha(\tilde{\lambda}) d\tilde{\lambda}}{\int_0^1 I(\tilde{\lambda})_{AM1.5} d\tilde{\lambda}} \qquad (A.2)$$

where: $I(\tilde{\lambda})_{AM1.5}$ is the Reference Solar Spectral Irradiance, fitted using the Boubaker Polynomials Expansion Scheme BPES:

$$I(\tilde{\lambda}) = \left[\frac{1}{2N_0} \sum_{n=1}^{N_0} \xi_n . B_{4n}(\tilde{\lambda} \times \beta_n) \right],$$

where β_n are the Boubaker polynomials B_{4n} minimal positive roots, ξ_n are given coefficients, N_0 is a given integer, and $\alpha(\tilde{\lambda})$ is the normalized absorbance spectrum.

The normalized absorbance spectrum $\alpha(\tilde{\lambda})$ is deduced from the BPES. According to this protocol, a set of *m* experimental measured values of the transmittance-reflectance vector

Full Paper

$\left(\mathbf{T}_i(\tilde{\lambda}_i); \mathbf{R}_i(\tilde{\lambda}_i)\right)\Big|_{i=1..m}$ versus the normalized wavelength

$\tilde{\lambda}_i\Big|_{i=1..m}$ is established. Then the system (A.3) is set:

$$\begin{cases} \mathbf{R}(\tilde{\lambda}) = \left[\dfrac{1}{2N_0}\sum_{n=1}^{N_0}\xi_n \times B_{4n}(\tilde{\lambda}\times\beta_n)\right] \\ \mathbf{T}(\tilde{\lambda}) = \left[\dfrac{1}{2N_0}\sum_{n=1}^{N_0}\xi_n' \times B_{4n}(\tilde{\lambda}\times\beta_n)\right] \end{cases} \quad \textbf{(A3)}$$

Where β_n are the 4n-Boubaker polynomials B_{4n} minimal positive roots, N_0 is a given integer and ξ_n and ξ_n' are coefficients determined through Boubaker Polynomials Expansion Scheme BPES.

Finally, the normalized absorbance spectrum $\alpha(\tilde{\lambda})$ is calculated using the relation (A.4):

$$\alpha(\tilde{\lambda}) = \frac{1}{d\sqrt{2}}\sqrt{\left|\mathbf{Ln}\frac{1-\mathbf{R}(\tilde{\lambda})}{\mathbf{T}(\tilde{\lambda})}\right| \times \left|\mathbf{Ln}\frac{\left(1-\mathbf{R}(\tilde{\lambda})\right)^2}{\mathbf{T}(\tilde{\lambda})}\right|} \quad \textbf{(A.4)}$$

where d is the layer thickness.

The effective absorptivity $\hat{\alpha}$ is calculated using robin (Eq. A.2) and (Eq. A.4).

CONCLUSION

WO$_3$ nano-films have been grown on glass substrates using an enhanced pyrolytic spray setup. The obtained films were subjected to sulfurisation under low pressure at 550°C. Transmittance spectra showed that thin films are transparent at the visible domain concordantly with the results recorded in recent literature. The predominance of the c-axis preferential orientation of the obtained compound (WS$_2$) has been verified by several means. This result is very stimulating since a relatively costless and simple spray pyrolysis technique can be used to prepare such binary materials and open the way of possible valorisation of the prepared films in many opto-electronic applications. Further studies are in progress to study the absorbance as well as the effects of gradually increased doping on the photoluminescence and the electrical conductivity of these WS$_2$ nano-films.

REFERENCES

[1] A.Amlouk, K.Boubaker, M.Amlouk; Alloys Compd., **490**, 602 **(2010).**

[2] A.Amlouk, K.Boubaker, El L.Mir, M.Amlouk; The Europ.Physical J.Applied Phys., **53**, 20502 **(2011).**

[3] A.Amlouk, K.B.B.Mahmoud ,M.Amlouk; Alloys Compd., **482,** 164 **(2009)**

[4] S.Belgacem, R.Bennaceur, J.Saurel, J.Bougnot; Rev Phys Appl, **25**, 1245 **(1990).**

[5] S.Belgacem, J.M.Saurel, J.Bougnot; Thin Solid Films, **92**, 199 **(1982).**

[6] K.Boubaker, M.Amlouk; Solar Energy, **84**, 1873 **(2010).**

[7] J.W.Chung, Z.R.Dai, F.S.Ohuchi; Cryst Growth, **186**, 137 **(1988).**

[8] J.J.Devadasan, C.Sanjeeviraja, M.Jayachandran; Cryst.Growth, **226**, 67 **(2001).**

[9] C.Feng, C.Huang, Z.Guo, H.Liu; Electrochemistry Communications, **9**, 119 **(2007).**

[10] S.Fridjine, M.Amlouk; Modern Physics Letters B, **23**, 2179 **(2009)**.

[11] S.Fridjine, K.Boubaker, M.Amlouk; Funct.Mat. Lett., **2,** 44 **(2009).**

[12] M.Genut, L.Margulis, R.Tenne, G.Hodes; Thin Solid Films, **219,** 30 **(1992).**

[13] A.Jager-Waldau E.Bucher; Thin Solid Films, **200**, 157 **(1991).**

[14] A.Jager-Waldau, M.L.Steiner, R.Jager-Waldau, R.Burkhart, E.Bucher; Thin Solid Films, **189**, 339 **(1990).**

[15] V.B.Kumar, D.Mohanta; Bull.Mater.Sci., **34**, 435 **(2011).**

[16] S.Kuwata, Y.Mizobe, M.Hidai; J.Chem.Soc.Dalton Trans., **10**, 1753 **(1997).**

[17] A.Levasseur, E.Schmidt, G.Meunier, D.Gonbeau, L.Benoist, G.Pfister-Guillouzo; Power Sources, **54**, 352 **(1995).**

[18] S.J.Li, J.C.Bernede, J.Pouzet, M.Jamali; Phys.Condens Matter, **8**, 2291 **(1996).**

[19] J.M.Martin, C.Donnet, T.LeMogne, T.Epicier; Phys.Rev.B, **48**, 10583 **(1993).**

[20] P.M.Martin; Handbook of Deposition Technologies for Films and Coatings (Third Edition), Elsevier Inc. **(2010).**

[21] I.Martin-Litas, P.Vinatier, A.Levasseur, J.C.Dupin, D.Gonbeau; J.Power Sources, **97-98,** 545 **(2001).**

[22] S.Miyake, Y.Sekine, J.Noshiro; Jap. Appl.Phys., **1**, 43, 4338

[23] B.Ouni, A.Boukhachem, S.Dabbous, A.Amlouk, K.Boubaker, M.Amlouk; Materials Science in Semi-conductor Processing, **13**, 281 **(2010).**

[24] P.S.Patil; Bull.Mater.Sci., **23**, 309 **(2000).**

Full Paper

[25] J.M.Patterson, J.M.Lightstone, G.Michael, M.G.White; Phys.Chem.A , **112**, **(2008).**

[26] S.V.Prasad, J.S.Zabinski; Mater.Sci.Lett., **12**, 1413 **(1993).**

[27] S.V.Prasad, N.T.Mcdevitt, J.S.Zabinski; Wear, **237**, 186 **(2000).**

[28] T.W.Scharf, S.V.Prasad, M.T.Dugger, P.G.Kotula, R.S.Goeke, R.K.Grubbs; Acta Mater, **54**, 4731 **(2006).**

[29] T.Tsirlina, S.Cohen, H.Cohen, L.Sapir, M.Peisach, R.Tennea, A.Matthaeus, S.Tiefenbacher, W.Jaegermann, E.A .Ponomarev, C.Lévy-Clément; Solar Energy Materials and Solar Cells, **44,** 457 **(1996).**